Brief communication : Evaluating Antarctic precipitation in ERA5 and CMIP6 against CloudSat observations

Marie-Laure Roussel [1], Florentin Lemonnier [1], Christophe Genthon [1], and Gerhard Krinner [2]

[1]Laboratoire de Météorologie Dynamique, Institut Pierre-Simon Laplace, Sorbonne Université / CNRS / École Normale Supérieure – PSL Research University / École Polytechnique – IPP, Paris, France
[2]Institut des Géosciences de l'Environnement, CNRS, Univ. Grenoble Alpes, 38000 Grenoble, France

Correspondence: (Marie-Laure Roussel (marie-laure.roussel@lmd.polytechnique.fr))

Abstract. CMIP5, CMIP6 and ERA5 antarctic precipitations are evaluated against CloudSat data. At continental and regional scales, ERA5 and CMIP models median are biased high, with insignificant improvement from CMIP5 to CMIP6 despite near-surface temperature improvement. However, less models yield outlying overestimation in CMIP6. AMIP configurations perform better than historical ones and, surprisingly, relative errors in areas of complex topography are higher (up to 50%) in
5 the 5 higher resolution models. The seasonal cycle is well reproduced by the median of the CMIP models but not by ERA5. There is limited progress from CMIP5 to CMIP6 and still room for improvement.

1 Introduction

Antarctica is the largest freshwater reservoir on Earth. Because of its sea-level equivalent of 57.9 ± 0.9 m (Morlighem et al., 2019), changes of the ice sheet mass balance can have important consequences for global sea level. Apart from a small con-
10 tribution from ice deposition, precipitation is by far the dominant positive term in the ice sheet mass balance, at equilibrium compensated for by meltwater drainage and ice discharge (e.g., Lenaerts et al., 2019). Precipitation is the main source of interannual mass balance variability of the ice sheet and is projected to increase in a warmer future (e.g., Krinner et al., 2008; Frieler et al., 2015). Therefore, an evaluation of the most recent CMIP6 coordinated climate model simulations (Eyring et al., 2016) is timely.

15 Over the last decades, numerous technical developments have led to an increased number of meteorological measurements. In this study, precipitation over almost the entire Antarctic continent is analysed at a climatological time scale using a large-scale snowfall data-set that is entirely independent from climate models, and thus provides the opportunity for objective evaluation. The reference for snowfall rate used here is the map produced by Palerme et al. (2014) based on the CloudSat satellite radar, which provided the first 4-year surface snowfall climatology for Antarctica. It has recently been followed by its complete
20 three-dimensional version (Lemonnier et al., 2019b). We use these satellite observations to assess the Antarctic precipitation rates simulated by the CMIP6 (World Climate Research Programme (WCRP) Coupled Model Intercomparison Project phase 6) models (Eyring et al., 2016) in diverse setups, at the continental and regional spatial scales, and at the annual and seasonal time scales. We further assess progress with respect to the preceding CMIP phase 5 (Taylor et al., 2012). ERA5 reanalyses are also used and evaluated in this comparison, because outputs are often used as a reference, particularly in less monitored areas,

25 and because of its foreseeable use as driver for regional climate models, the continental and climatological precipitation rates
of which are strongly determined by the driving global model (e.g., Di Luca et al., 2012).

2 Data and methods

2.1 Data

2.1.1 Snowfall : CloudSat radar

30 The instrument on the CloudSat satellite platform is a RADAR operating at 94GHz and looking at nadir. The Cloud Profiling
Radar (CPR) measures the back-scattered signal of hydrometeors. Based on micro-physical parameters (Wood et al., 2015)
and the diffusion properties of the ice particles, the snowfall rate can be computed. Constrained by the satellite orbit, this
measurement can be performed up to 82°S. Many sources of error are related to this measurement: the various assumptions
as well as the low frequency of passage of the satellite on the Antarctic induce uncertainties. (Lemonnier et al., 2019a) study
35 allowed to improved confidence in the CPR snowfall retrieval over peripheral areas by a comparison with *in-situ* measure-
ments (within maximum 25% error). In this work, we use data from the 2007-2010 Antarctic three-dimensional climatology
(Lemonnier et al., 2019b) yielding the vertical distribution of the snowfall rate with a resolution of 1° latitude and 2° longitude
- optimizing the agreement with *in-situ* observations (Souverijns et al., 2018; Palerme et al., 2014). Recently the need to take
into consideration the effect of soil echoes has been highlighted (Palerme et al., 2019), because it affects the measurement of
40 CPR especially in the areas of complex topography, such as mountains and fjords. Some abnormal values are ignored in this
dataset, but not highly impacting averages. Here we consider the radar information at the level of 1200 meters above ground
level to assess the surface snowfall rate.

2.1.2 Surface air temperature: SCAR Reader data

Changes in the quality of the representation of observed precipitation rates are briefly assessed in the light of temperature biases
45 with respect to SCAR Reader AWS and manned station data (Turner et al., 2004). For each station and model, we identified the
nearest grid point and used a spatial regression (based on the neighboring grid points) of surface temperature against surface
altitude in order to correct for altitude differences between the model and the observations. SCAR Reader data were used only
when at least 10 years of observations were available, and the model output was averaged over the number of years of available
observations, centered around the mean year of these observations between 1979 and 2005 (in order to evaluate progress from
50 CMIP5 to CMIP6).

2.1.3 CMIP5 and CMIP6 global climate models

The Coupled Model Intercomparison Project (CMIP, Taylor et al., 2012; Eyring et al., 2016) is coordinated by the World
Climate Research Programme (WCRP). Its main objective is to improve modeling and future predictions combining the natural
variability of the climate system and its response to modification of the radiative forcing in coordinated experiments (see

55 https://es-doc.org/cmip6-experiments/). The available model outputs taken into account in this study are listed in table A1 of the Appendix A. CMIP, which started in 1995, is currently in its 6th phase.

Here we evaluate CMIP5 and CMIP6 model output from the *amip* and *historical* experiments. *amip* is the configuration of the atmospheric circulation used when observed sea surface temperatures (SST) and sea ice (from 1979 to 2014) are selected as forcing. *historical* simulations are coupled ocean-atmosphere experiments. In both setups, observed time-varying atmospheric

60 composition (anthropogenic, natural and volcanic influences), solar forcing, land use etc. based on observations are prescribed. In addition, *highresSST-present*, defined in the framework of HighResMIP (Haarsma et al., 2016), is a configuration available in the CMIP6 archive similar to *amip* with forced SST, but with a higher horizontal resolution. The experiment is designed to allow evaluating the sensitivity of climate model output to spatial resolution, and to help understanding the origins of model biases. The historical CMIP6 model outputs, driven by observed boundary conditions, end in 2014, while the observational

65 period ended in 2005 in the earlier CMIP5 exercise. We therefore preferentially restrain the CMIP5 output to before 2005, complementing them by output from the RCP8.5 scenario run until 2014 where appropriate (see figure C1), because the realized CO_2 emissions between 2006 and 2014 closely follow those of that high emission scenario (Hayhoe et al., 2017). The start of our analysis period is 1979, corresponding to the beginning of the satellite period. We use all available CMIP5 and CMIP6 model, although it is well known (e.g., Masson and Knutti, 2011) that models managed by the same group or sharing a

70 common development history yield very similar output, potentially biasing multi-model means. We preferentially use median model output, which is less sensitive to such effects, and quantify inter-model dispersion by the 25 and 75% percentiles, which are insensitive to outliers. Furthermore, although the *highresSST-present* multi-model ensemble of opportunity contains several versions of most models at low and high resolution, we do not restrain our choice to the high-resolution model versions; nevertheless, on average, the *highresSST-present* ensemble of opportunity used here has, on average, a substantially higher

75 resolution than the *amip* and *historical* CMIP6 ensembles.

2.1.4 ERA5 reanalyses

ERA5 (Copernicus Climate Change Service (C3S), 2017) is the latest global reanalysis of the atmosphere made by the European Centre for Medium-Range Weather Forecasts (ECMWF) based on historical observation data since 1979 with the Integrated Forecasting System (IFS) model and its data assimilation system. Outputs from these reanalyses have high spa-

80 tial horizontal and vertical resolutions (30 kilometers, 137 vertical levels). In this work, the monthly averages of the ERA5 reanalyses are used for the 40 years from 1979 to 2018.

2.2 Methods

For precipitation, we consider the entire Antarctic ice sheet, including ice shelves, where CloudSat satellite observations are available (i.e. north of 82°S). In order to evaluate the performances of the models to reproduce the various precipitation regimes

85 of Antarctica, we examine both regional and seasonal averages. We consider the four standard meteorological seasons that are December-January-February (DJF), March-April-May (MAM), June-July-August (JJA) and September-October-November (SON). These are studied separately on the plateau (all areas above 2250 meters) and or serveral peripheral and intermediate

regions (defined by latitude and longitude, and an altitude lower than 2250 meters), as there are some seasonal signature differ-
ences mostly due to the sea-ice and the circumpolar current variations during the year with significant impact on precipitation

90 patterns on the ice sheet margin (Palerme et al., 2017) . Six regions have been selected based on latitude, longitude and alti-
tude to distinguish main geographical patterns : Plateau, East Antarctic Coast, the Peninsula, the Filchner-Ronne and Ross Ice
Shelves, and the remaining part of the West Antarctic Ice Sheet. These are shown in figure 1 and described in Appendix B.
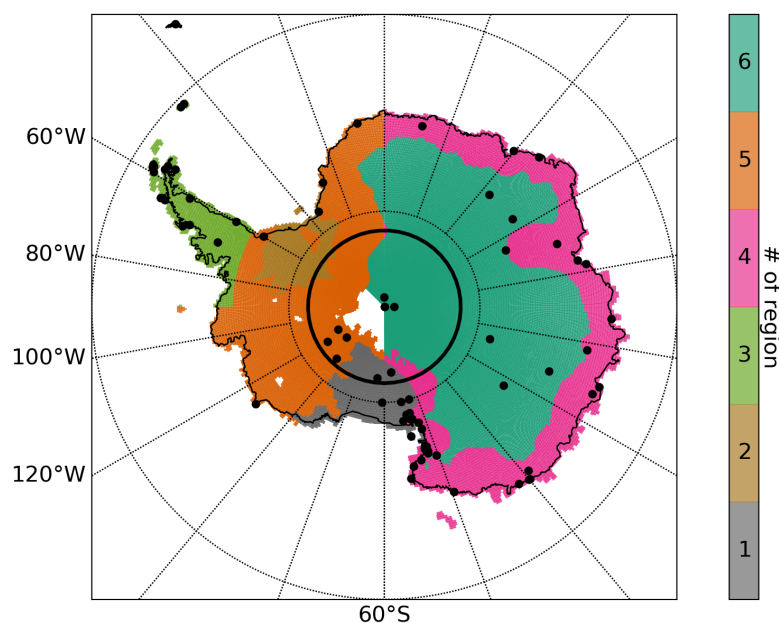
Figure 1. Map of the studied regions on the ERA5 grid. Numbers refer to the regions defined in table B1. Black dots indicate SCAR Reader
temperature measurement stations (AWS and manned stations). The black line indicates the 82°S latitude circle.

    To test the sensitivity of our conclusions concerning ERA and the CMIP outputs to the relatively short Four-year CloudSat
period, we compare the CloudSat 4-year time series with multiple time periods of the same length extracted from the 40-year

95 climatology of ERA5 and with the average of the 2007-2010 CloudSat period. We made 20 draws of 4 random years to process
the samples for the evaluation against the 2007-2010 CloudSat period. This number of 20 samples has been chosen because
there is no significant difference in the results with more samples. As we will show below (see section 2.3.1), our conclusions
are not very sensitive to these choices.

    Furthermore, as historical CMIP5 outputs are only available for years up to 2005, a direct comparison from 2007 to 2010

100 is not possible between CMIP5 and CloudSat. Annual mean snowfall (averaged over the whole Antarctic continent north of
82°S) starting in 1979 is available until 2005 for CMIP5, until 2014 for CMIP6, and until 2018 for ERA5. Over this period,
there is a slight positive mean precipitation trend in the CMIP ensembles (strongest, about 2% per decade, in the CMIP5 and
CMIP6 *historical* simulations), but the variations induced by this trend over the model periods are substantially weaker than

the absolute differences between the model means and the CloudSat observational average. Therefore, and because our results
are not particularly sensitive to the choice of model years, CMIP output is averaged over the entire respective simulation period
for comparison with CloudSat.

2.3 Results

2.3.1 Continent-wide climatological snowfall rates

Figure 2 displays the annual precipitation for the entire continent ("All") and the defined regions for CloudSat, ERA5 (both
the 2007-2010 period and the average of 20 draws of four random years with associated standard deviation) and the various
CMIP5 and CMIP6 ensembles. For all CMIP experiments, the ensemble median of the continental mean precipitation is above
the 2007-2010 CloudSat average of 186 mm water equivalent per year. Following (Palerme et al., 2017) who compared CMIP5
models to CloudSat snowfall measurements, we have identified CMIP5 and CMIP6 models that have continent-wide mean
snowfall rates within 20% of the CloudSat average value of 186 mm water equivalent per year, that is, between 150 and 223
mm per year. Not a single CMIP5 and CMIP6 model falls below this lower bound. Conversely, a substantial fraction of CMIP
models, both in CMIP5 and CMIP6, exceeds the upper bound of 223 mm per year. As a result, only 58% of the CMIP6 *amip*
models fall within the ±20% range around the CloudSat value, and this number decreases to 38% for CMIP6 *highresSST-
present*, the other ensembles lying between these extreme values. The atmosphere-only *amip* runs less frequently exceed the
±20% bound (56% and 58% within the 20% range for CMIP5 and CMIP6, respectively) than the coupled *historical* runs (43%
and 48% within the 20% range for CMIP5 and CMIP6, respectively). We must note that the median model precipitation rate
shows no improvement from CMIP5 to CMIP6; if anything, compared to CMIP5, there is even a degradation in the CMIP6
median *historical* simulation with respect to CloudSat.

There is therefore a systematic high bias, exacerbated a higher spatial resolution, and no substantial improvement is obvious
on the continental scale from CMIP5 to CMIP6; prescribed observed oceanic boundary conditions (SST and sea ice) in the
amip runs lead, unsurprisingly, to more realistic simulated precipitation rates than in the corresponding coupled runs.

From CMIP5 to CMIP6, one can note, positively, that the number of models with extreme positive precipitation biases is
reduced. In the CMIP5 *historical* ensemble, for example, 4 models exceed (in one case very substantially) the maximum of the
CMIP6 ensemble at 353 mm, which is almost twice the observed 2007-2010 rate.

Interestingly, ERA5 similarly exhibits a positive mean precipitation bias of about 30 mm per year, and is therefore not better,
at least compared to the CloudSat climatology, than the CMIP5 and CMIP6 median models.

2.3.2 Regional averages

Figure 2 shows that ERA5 and the CMIP6-highresSST models, which have higher horizontal resolutions that should enable
a better spatial representation of the small scale processes, particularly those induced by topography, do not exhibit reduced
errors in the Peninsula region and in West Antarctica (regions named LowWest, Filchner and Ross). Relative errors with respect
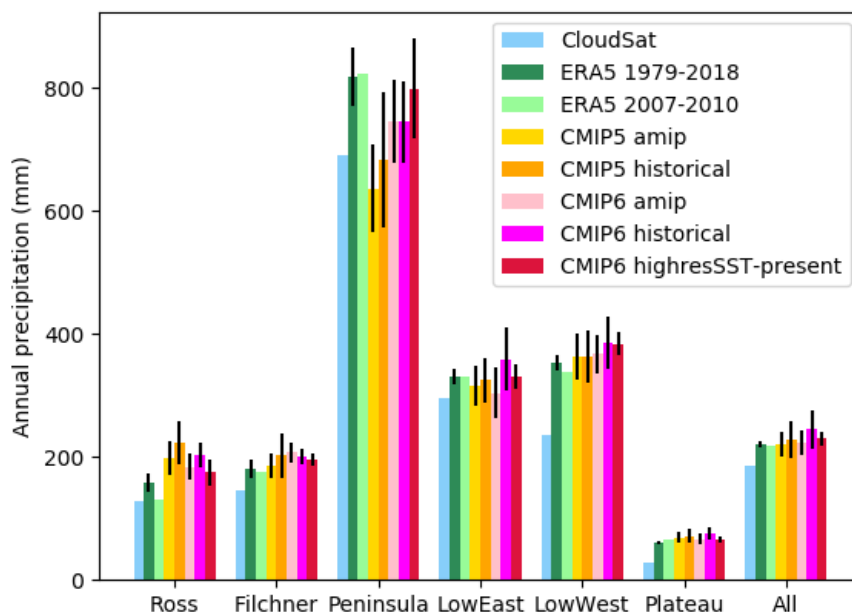
Figure 2. Average snowfall rate per region and for the entire continent north of 82°S for CloudSat (blue, 2007-2010), ERA5 (computed on 20 draws of 4 random years between 1979 and 2018, with standard deviation, and the 2007-2010 average), and the various CMIP ensembles. For CMIP, the ensemble medians and the 25th and 75th percentiles are indicated.

135   to the CloudSat measurement can exceed 50% in these regions, compared to the lower regions of East Antarctica (LowEast) where it is as low as a few percents.

    Conspicuously, all CMIP ensembles and ERA5 exhibit positive biases with respect to CloudSat in all regions. The strongest relative biases are located in the Plateau region, that is, above 2250 m, where theCloudSat mean is about 29 mm of water equivalent per year, while the ERA mean for the same period is 65 mm per year, and the CMIP ensembles have even stronger

140   biases. In most regions, the *amip* simulations exhibit lower biases than the coupled *historical* simulations in the CMIP5 and CMIP6 ensembles, as already seen for the continental mean values.

    There is no clear overall improvement in the performance of the CMIP6 ensemble over the CMIP5 ensemble. There is degradation in some regions (for example the Peninsula) and improvement in others, such as the Plateau region, where the improvement in the *amip* configuration is modest (see also Figure 3), but important because of the large spatial extent of

145   the East Antarctic Plateau, and on the Ross Ice Shelf. In dry these plateau and ice shelf areas, the *highresSST-present* runs consistently performs better than the other CMIP6 runs. This is contrary to expectations that higher spatial resolution, allowing a better representation of topographical effects, would principally allow better representing precipitation rates in regions with steep topography, that is, mostly coastal areas.

2.3.3 Seasonal averages

150 Figure 3 displays the observed and simulated seasonal variations of precipitation separately for the high (>2250 m) and low (<2250 m) regions of the continent. The CMIP ensembles capture the weak annual cycle in the plateau regions, characterized by a maximum in DJF and a minimum in SON, but, as reported above, they overestimate the average precipitation rate substantially. ERA5 does not capture this seasonality and simulated maximum precipitation rates in MAM and JJA. In the lower reaches of the continent, the CMIP ensembles and ERA5 do capture the observed seasonality, with maximum precipitation

155 rates typically in MAM. This is very probably linked to the availability of oceanic moisture, driven by sea ice around the continent and the delayed annual temperature cycle in the Southern Ocean, and to the seasonality of meriodional atmospheric circulation (Genthon and Krinner, 1998).

3 Discussion and conclusion

The CloudSat precipitation climatology provides the possibility to evaluate climate models and reanalyses against model-
160 independent satellite-derived data. By comparing ERA5 reanalysis output from multiple random 4-year periods against output for the 4-year observational period (2007-2010) and the satellite-derived data, we have shown that on regional scales, a 4-year period is long enough to draw robust conclusions about misfits between the models and the satellite data set.

The main results of this short study are that: 1) All CMIP model ensemble medians and ERA5 overestimate the continental mean precipitation rates; 2) The positive biases are particularly strong in the plateau regions; 3) There is no measurable
165 improvement, in terms of continental and regional mean precipitation rates and their seasonality, from CMIP5 to CMIP6; 4) The seasonal cycle of precipitation, both on the plateau and lower (coastal) regions, is reasonably well captured by the median CMIP models; 5) Median precipitation rates tend to be better reproduced in the atmosphere-only *amip* configurations than in the coupled *historical* setups; 6) Positive precipitation biases in particular in the Peninsula region are exacerbated at higher resolution in the *higtresSST-present* ensemble; 7) The CMIP6 ensemble suffers less than CMIP5 from outliers with very
170 strong positive precipitation biases.

It is interesting to note that although there is no progress in the representation of large-scale mean precipitation and of its seasonality from CMIP5 to CMIP6, there is a concomitant measurable progress in the representation of surface air temperature. Regional-scale multi-model median root-mean square errors are reduced by typically 5 to 10% between these successive CMIP generations (see D1 in the annex). Conversely, this indicates that an improved simulation of near-surface temperature does not
175 necessarily lead to an improved representation of precipitation-generating processes.

Author contributions. This research was designed by all authors. MLR wrote the initial draft and all coauthors contributed to the writing.

Competing interests. The authors declare no competing interests.
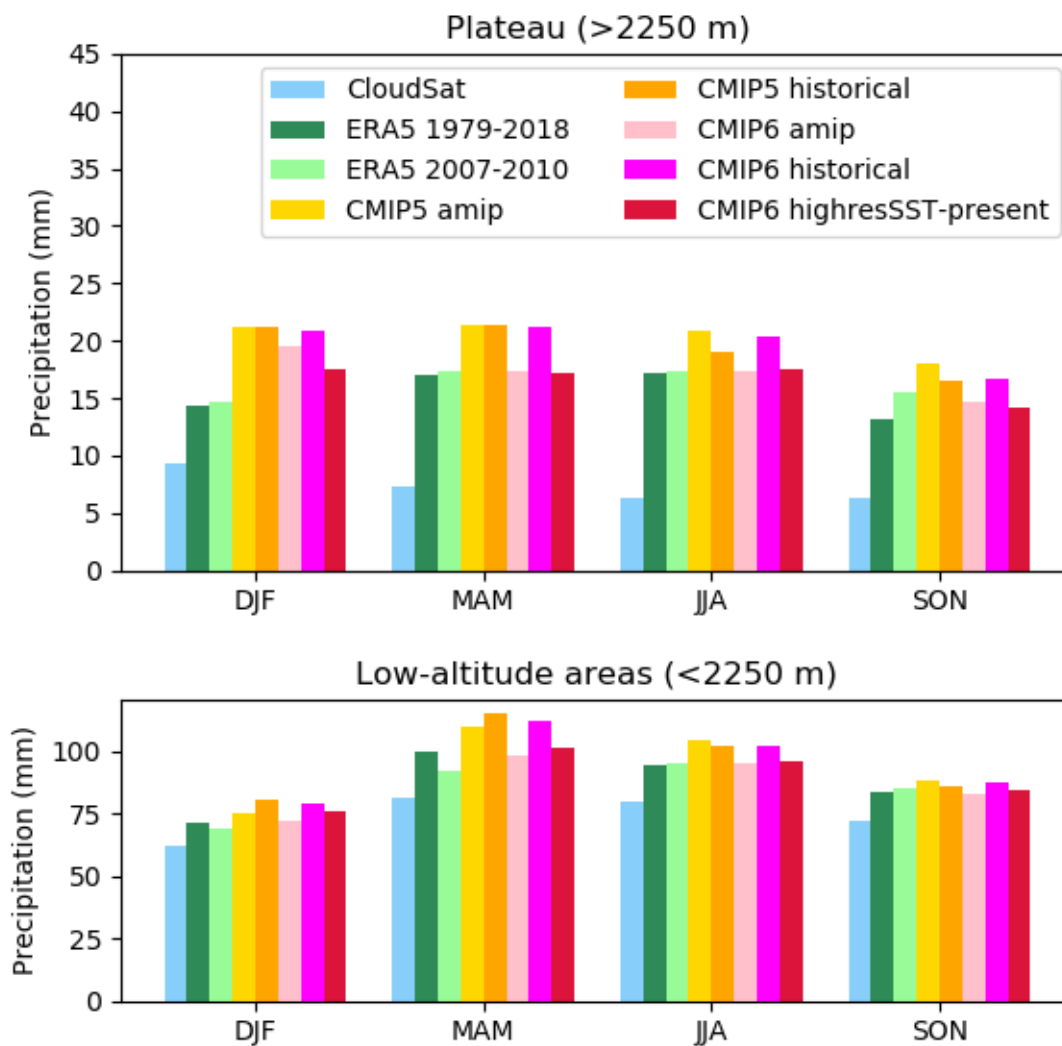
Figure 3. Seasonal averages of the observed mean 2007-2010 CloudSat, mean ERA 5 (random and 2007-2010 averages), and ensemble median long-term average CMIP5 and CMIP6 snowfall rates per season for the plateau areas (top) and the low-lying reaches of the continent (bottom).

Acknowledgements. This paper is a contribution to the APRES3 project supported by the French polar institute IPEV and the French national research fund ANR. Support by the French space agency CNES for program EECLAT is also acknowledged. MLR benefits a PhD grant by Ecole Polytechnique.

180

References

Copernicus Climate Change Service (C3S): ERA5: Fifth generation of ECMWF atmospheric reanalyses of the global climate, dataset available from https://cds.climate.copernicus.eu/cdsapp, 2017.

Di Luca, A., de Elía, R., and Laprise, R.: Potential for added value in precipitation simulated by high-resolution nested regional climate models and observations, Climate Dynamics, 38, 1229–1247, 2012.

Eyring, V., Bony, S., Meehl, G. A., Senior, C. A., Stevens, B., Stouffer, R. J., and Taylor, K. E.: Overview of the Coupled Model Intercomparison Project Phase 6 (CMIP6) experimental design and organization, Geoscientific Model Development (Online), 9, 2016.

Frieler, K., Clark, P. U., He, F., Buizert, C., Reese, R., Ligtenberg, S. R., Van Den Broeke, M. R., Winkelmann, R., and Levermann, A.: Consistent evidence of increasing Antarctic accumulation with warming, Nature Climate Change, 5, 348, 2015.

Genthon, C. and Krinner, G.: Convergence and Disposal of Energy and Moisture on the Antarctic Polar Cap from ECMWF Reanalyses and Forecasts, Journal of Climate, 11, 1703–1716, https://doi.org/10.1175/1520-0442(1998)011<1703:CADOEA>2.0.CO;2, 1998.

Haarsma, R. J., Roberts, M. J., Vidale, P. L., Senior, C. A., Bellucci, A., Bao, Q., Chang, P., Corti, S., Fučkar, N. S., Guemas, V., von Hardenberg, J., Hazeleger, W., Kodama, C., Koenigk, T., Leung, L. R., Lu, J., Luo, J.-J., Mao, J., Mizielinski, M. S., Mizuta, R., Nobre, P., Satoh, M., Scoccimarro, E., Semmler, T., Small, J., and von Storch, J.-S.: High Resolution Model Intercomparison Project (HighResMIP v1.0) for CMIP6, Geoscientific Model Development, 9, 4185–4208, https://doi.org/10.5194/gmd-9-4185-2016, https://www.geosci-model-dev.net/9/4185/2016/, 2016.

Hayhoe, K., Edmonds, J., Kopp, R., LeGrande, A., Sanderson, B., Wehner, M., and Wuebbles, D.: Climate models, scenarios, and projections, in: ClimateScience Special Report: A Sustained Assessment Activity of the U.S. Global Change Research Program, edited by Wuebbles, D., Fahey, D., Hibbard, K., Dokken, D.J. andStewart, B., and Maycock, T., 589, pp. 186–227, U.S. Global Change Research Program, Washington, DC, USA, https://digitalcommons.unl.edu/usdeptcommercepub/589, 2017.

Krinner, G., Guicherd, B., Ox, K., Genthon, C., and Magand, O.: Influence of oceanic boundary conditions in simulations of Antarctic climate and surface mass balance change during the coming century, Journal of Climate, 21, 938–962, 2008.

Lemonnier, F., Madeleine, J.-B., Claud, C., Genthon, C., Duran-Alarcon, C., Palerme, C., Berne, A., Souverijns, N., Van Lipzig, N., Gorodetskaya, I., et al.: Evaluation of CloudSat snowfall rate profiles by a comparison with in situ micro-rain radar observations in East Antarctica, Cryosphere, 13, 943–954, 2019a.

Lemonnier, F., Madeleine, J.-B., Claud, C., Palerme, C., Genthon, C., L'Ecuyer, T., and Wood, N. B.: CloudSat-inferred vertical structure of precipitation over the Antarctic continent, https://doi.org/10.1029/2019JD031399, 2019b.

Lenaerts, J. T. M., Medley, B., van den Broeke, M. R., and Wouters, B.: Observing and Modeling Ice Sheet Surface Mass Balance, Reviews of Geophysics, 57, 376–420, https://doi.org/10.1029/2018RG000622, https://agupubs.onlinelibrary.wiley.com/doi/abs/10.1029/2018RG000622, 2019.

Masson, D. and Knutti, R.: Climate model genealogy, Geophysical Research Letters, 38, 2011.

Morlighem, M., Rignot, E., Binder, T., Blankenship, D., Drews, R., Eagles, G., Eisen, O., Ferraccioli, F., Forsberg, R., Fretwell, P., et al.: Deep glacial troughs and stabilizing ridges unveiled beneath the margins of the Antarctic ice sheet, Nature Geoscience, pp. 1–6, 2019.

Palerme, C., Kay, J., Genthon, C., L'Ecuyer, T., Wood, N., and Claud, C.: How much snow falls on the Antarctic ice sheet?, The Cryosphere, 8, 1577–1587, 2014.

Palerme, C., Genthon, C., Claud, C., Kay, J. E., Wood, N. B., and L'Ecuyer, T.: Evaluation of current and projected Antarctic precipitation in CMIP5 models, Climate dynamics, 48, 225–239, 2017.

Palerme, C., Claud, C., Wood, N. B., L'Ecuyer, T., and Genthon, C.: How does ground clutter affect CloudSat snowfall retrievals over ice sheets?, IEEE Geoscience and Remote Sensing Letters, 16, 342–346, 2019.

220 Souverijns, N., Gossart, A., Lhermitte, S., Gorodetskaya, I. V., Grazioli, J., Berne, A., Duran-Alarcon, C., Boudevillain, B., Genthon, C., Scarchilli, C., et al.: Evaluation of the CloudSat surface snowfall product over Antarctica using ground-based precipitation radars, Cryosphere, 12, 3775–3789, 2018.

Taylor, K. E., Stouffer, R. J., and Meehl, G. A.: An overview of CMIP5 and the experiment design, Bulletin of the American Meteorological Society, 93, 485–498, 2012.

225 Turner, J., Colwell, S. R., Marshall, G. J., Lachlan-Cope, T. A., Carleton, A. M., Jones, P. D., Lagun, V., Reid, P. A., and Iagovkina, S.: The SCAR READER project: toward a high-quality database of mean Antarctic meteorological observations, Journal of Climate, 17, 2890–2898, 2004.

Wood, N. B., L'Ecuyer, T. S., Heymsfield, A. J., and Stephens, G. L.: Microphysical Constraints on Millimeter-Wavelength Scattering Properties of Snow Particles, Journal of Applied Meteorology and Climatology, 54, 909–931, https://doi.org/10.1175/JAMC-D-14-0137.1,
230 https://doi.org/10.1175/JAMC-D-14-0137.1, 2015.

Appendix A: CMIP5 & CMIP6 version models

CMIP5	
amip	ACCESS1-0, ACCESS1-3, bcc-csm1-1-m, bcc-csm1-1, BNU-ESM CCSM4, CESM1-CAM5, CMCC-CM, CNRM-CM5, CSIRO-Mk3-6-0, EC-EARTH, FGOALS-g2, FGOALS-s2, GFDL-CM3, GISS-E2-R inmcm4, IPSL-CM5A-LR, IPSL-CM5A-MR, IPSL-CM5B-LR, MIROC-ESM MIROC5, MPI-ESM-LR, MPI-ESM-MR, MRI-CGCM3, NorESM1-M
historical	ACCESS1-0, ACCESS1-3, bcc-csm1-1-m, bcc-csm1-1, BNU-ESM, CanCM4, CanESM2, CCSM4, CESM1-BGC, CESM1-CAM5, CESM1-FASTCHEM, CESM1-WACCM, CMCC-CESM, CMCC-CMS, CNRM-CM5-2, CNRM-CM5, CSIRO-Mk3-6-0, CSIRO-Mk3L-1-2, EC-EARTH, FGOALS-g2, FGOALS-s2, FIO-ESM, GFDL-CM2p1, GFDL-CM3, GFDL-ESM2G, GFDL-ESM2M, GISS-E2-H-CC, GISS-E2-H, GISS-E2-R-CC, GISS-E2-R, HadCM3, HadGEM2-AO, HadGEM2-CC, HadGEM2-ES, inmcm4, IPSL-CM5A-LR, IPSL-CM5A-MR, IPSL-CM5B-LR, MIROC-ESM-CHEM MIROC-ESM, MIROC4h, MIROC5, MPI-ESM-LR, MPI-ESM-MR, MPI-ESM-P, MRI-CGCM3, MRI-ESM1, NorESM1-M, NorESM1-ME
CMIP6	
amip	BCC-CSM2-MR, BCC-ESM1, CAMS-CSM1-0, CanESM5, CESM2-WACCM CESM2, CNRM-CM6-1, CNRM-ESM2-1, E3SM-1-0, EC-Earth3-Veg, EC-Earth3, FGOALS-f3-L, GFDL-CM4, GFDL-ESM4, GISS-E2-1-G, HadGEM3-GC31-LL, INM-CM5-0, IPSL-CM6A-LR, MIROC6, MRI-ESM2-0, NESM3, NorCPM1, NorESM2-LM, SAM0-UNICON, UKESM1-0-LL
historical	BCC-CSM2-MR, BCC-ESM1, CAMS-CSM1-0, CanESM5, CESM2-WACCM, CESM2, CNRM-CM6-1-HR, CNRM-CM6-1, CNRM-ESM2-1, E3SM-1-0, EC-Earth3-Veg, EC-Earth3, FGOALS-g3, GFDL-CM4, GFDL-ESM4, IPSL-CM6A-LR, GISS-E2-1-G, GISS-E2-1-H, HadGEM3-GC31-LL, INM-CM4-8, MIROC-ES2L, MIROC6, MRI-ESM2-0, NESM3, NorCPM1, NorESM2-LM, SAM0-UNICON, UKESM1-0-LL
highresSST	CMCC-CM2-HR4, CMCC-CM2-VHR4, CNRM-CM6-1-HR, CNRM-CM6-1, ECMWF-IFS-HR, ECMWF-IFS-LR, FGOALS-f3-H, FGOALS-f3-L, GFDL-CM4C192, HadGEM3-GC31-HM, HadGEM3-GC31-LM, HadGEM3-GC31-MM, INM-CM5-H, IPSL-CM6A-ATM-HR, IPSL-CM6A-LR, MPI-ESM1-2-HR, MPI-ESM1-2-XR, MRI-AGCM3-2-H, MRI-AGCM3-2-S, NICAM16-7S, NICAM16-8S

Table A1. CMIP5 and CMIP6 models considered in this study

Appendix B: Geographical delimitations for the regional analysis

Regions	1 : Ross	2 : Filchner	3 : Peninsula	4 : LowEast	5 : LowWest	6 : Plateau
Latitude	-99°,-75°	-99°,-76°	-74°,-59°	-99°,-59°	-99°,-59°	-99°,-59°
Longitude	150°,240°	270°,340°	270°,320°	0°,180°	180°,360°	0°,360°
Altitude	< 300m	< 300m	-	< 2250m	< 2250m	> 2250m

Table B1. Selection criteria applied to define the studied regions.

Appendix C: CMIP5, CMIP6, ERA5 and CloudSat time series of mean annual surface precipitation rates
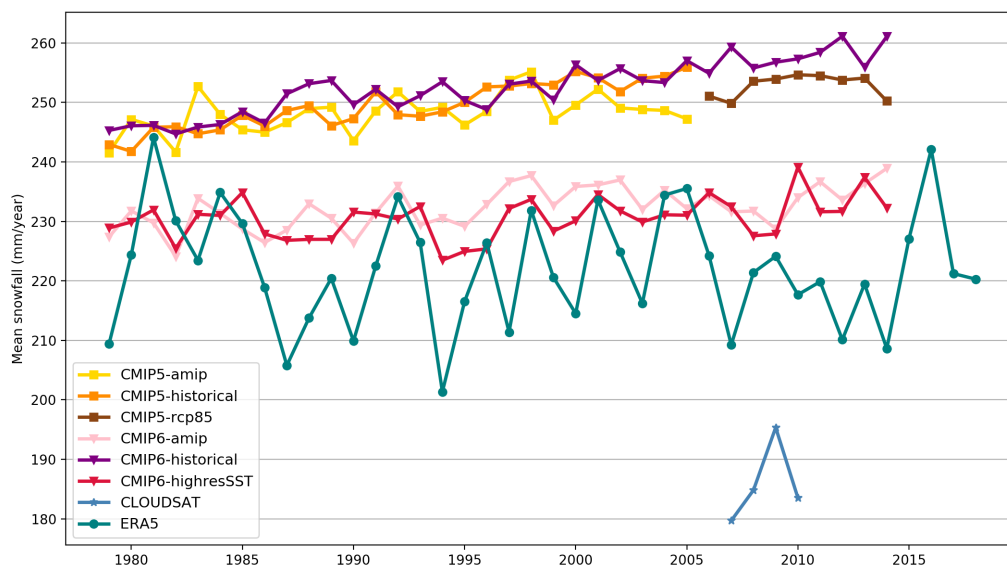
Figure C1. 1979 to 2018 time series of mean annual snowfall rate over the entire Antarctic continent. The average values for all the models of each CMIP (5 & 6) version are plotted and the standard deviations are represented by the colored bands. Blue and green lines are respectively CloudSat and ERA5 annual mean values.

Appendix D: CMIP5 & CMIP6 surface air temperature comparison to SCAR Reader stations
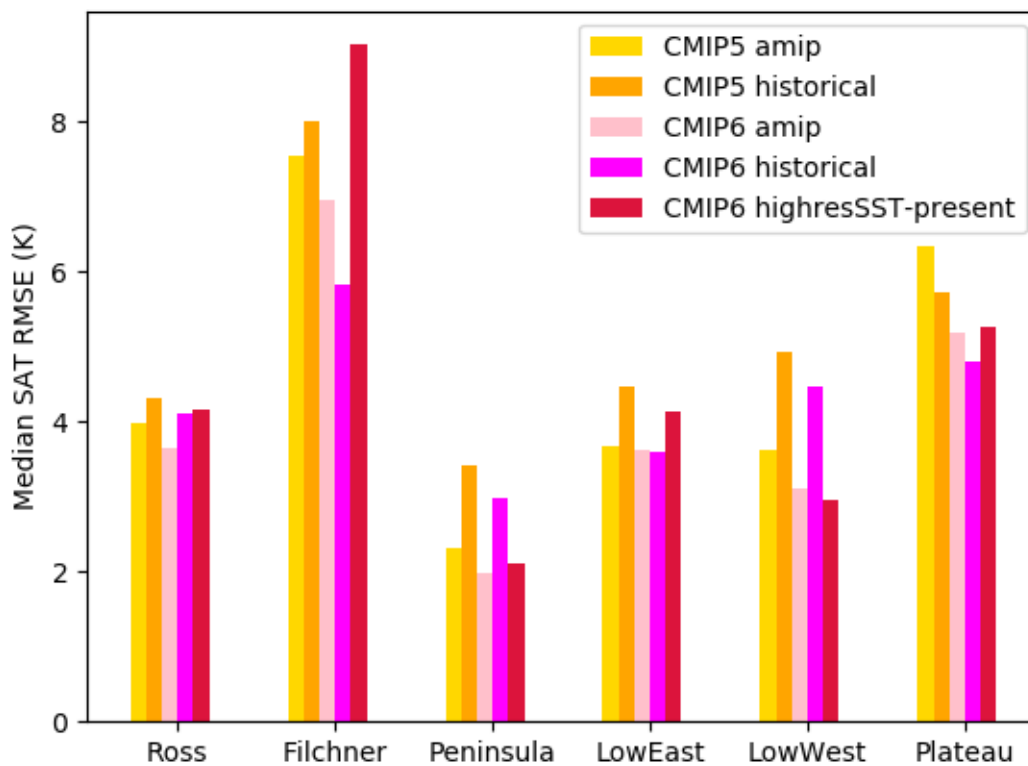
Figure D1. Multi-model median of the multi-station mean root-mean square error (RMSE, in K) of simulated monthly surface air temperatures against SCAR Reader stations (AWS and manned), for the different regions.